Natalia WIERZBICKA*, Rafał TALAR**

TRIBOLOGICAL PROPERTIES OF A SILICONE-BASED COMPOSITE WITH INORGANIC ADDITIVES

WŁAŚCIWOŚCI TRIBOLOGICZNE KOMPOZYTU NA OSNOWIE SILIKONOWEJ Z NIEORGANICZNYMI DODATKAMI

Key words:	coefficient of friction, wear, silicone, hexagonal boron nitride, titanium.
Abstract:	The paper presents the results of experimental studies, including tribological tests of silicone-based composites with additions of hexagonal boron nitride (hBN) and titanium (Ti). The tests were conducted on a Bruker UMT2 tribotester and using a pin-on-disk setup developed by the authors, without a lubricating medium, and they employed a steel ball made of 100Cr6 steel and a sample made of the composite. During the tests, the products were not removed from the contact area. The paper analyzes the influence of additives on the tribological properties of the composite, i.e., the coefficient of friction (COF) as a function of distance and the wear of the tested samples. In the case of samples containing hBN, the COF decreases with an increase in its content. After reaching a volumetric percentage concentration of 20%, it begins to stabilize with the increase in mass loss. The profiles of COF changes as a function of distance for samples with different additive contents are comparable. The self-lubricating properties of hBN have been confirmed. The addition of Ti reduces the COF value, which decreases with the increase in the Ti content. Samples with a mass percentage concentration exceeding 100% of the Ti content have a COF value equal to the initial value for silicone. The composite containing hBN has a lower COF value than samples with the Ti addition, and the wear tracks on their surface are narrower and shallower. The article is published in connection with the Autumn Tribology School.
Słowa kluczowe:	współczynnik tarcia, zużycie, silikon, heksagonalny azotek boru, tytan.
Streszczenie:	W pracy zostały przedstawione wyniki badań doświadczalnych obejmujących testy tribologiczne kompozytów na osnowie silikonowej z dodatkami heksagonalnego azotku boru (hBN) i tytanu (Ti). Badania przeprowadzono na tribotesterze Bruker UMT2 i stanowisku autorskim typu Pin-on-disk bez stosowania medium smarującego w skojarzeniu kulki stalowej wykonanej ze stali 100Cr6 i próbki wykonanej z kompozytu. W trakcie prowadzenia badań produkty nie były usuwane ze strefy ruchu. W pracy analizowano wpływ dodatków na właściwości tribologiczne kompozytu, tj. wyznaczono współczynnik tarcia (COF) w funkcji drogi oraz zużycie badanych próbek. W przypadku próbek zawierających hBN wartość COF maleje wraz ze wzrostem jego zawartości. Po osiągnięciu stężenia procentowego objętościowego o wartości 20% zaczyna się stabilizować wraz ze wzrostem ubytku masy. Przebiegi zmian COF w funkcji drogi dla próbek o różnej zawartości dodatku są porównywalne. Właściwości samosmarujące hBN zostały potwierdzone. Dodatek Ti powoduje obniżenie wartości COF, która maleje wraz ze wzrostem zawartości dodatku Ti. Próbki o stężeniu procentowym masowym przekraczającym 100% zawartości Ti posiadają wartość COF równą początkowej dla silikonu. Kompozyt zawierający hBN charakteryzuje się mniejszą wartością COF niż próbki z dodatkiem Ti, a ścieżki powstałe na ich powierzchni są węższe i płytsze. Artykuł publikowany w związku z Jesienną Szkołą Tribologiczną.

*   ORCID: 0000-0002-4862-6534. Poznan University of Technology, Faculty of Mechanical Technology, M. Skłodowska-Curie Square 5, 60-965 Poznań, Poland, e-mail: natalia.wierzbicka@put.poznan.pl

**   ORCID: 0000-0003-4355-9923. Poznan University of Technology, Faculty of Mechanical Technology, M. Skłodowska-Curie Square 5, 60-965 Poznań, Poland.

INTRODUCTION

Tribology is a field of science that deals with the study of interactions between surfaces in contact and phenomena associated with them, such as friction, wear, and lubrication. In the case of soft surfaces sliding against hard surfaces, phenomena such as the Schallamach wave can occur, especially at low pressures and low sliding velocities [L. 1]. In such cases, stick-slip instabilities often occur, which in certain configurations can transform into wave-like motions and surface wrinkling. These waves can cause vibrations, noise, structural wear, and leakage of seals in machine components such as seals, sliding elements, tires, or conveyor belts. Therefore, intensive efforts are made to prevent or predict these negative effects. To this end, knowledge of these processes is constantly expanding, and various structures, coatings, or lubricants are applied to mitigate these effects [L. 2, 3].

M. Scherge and S. Gorb introduced basic tribological descriptions for micro- and nanotribology structures, which are still used. They describe, among other things, the relationship between velocity and friction in stick-slip processes, the influence of adhesion, capillary forces, and viscoelastic properties, the description of interactions using energy, and the influence of topography on friction characteristics. In their work, they already described stick-slip processes on a nanometric scale and defined a critical velocity, which is inversely proportional to the sliding time. They focused, among other things, on the adhesive function of insect feet on smooth surfaces [L. 4–6].

To change the friction characteristics using nanostructured surfaces, various possibilities can be used, depending on the flexibility, interaction energy, latches, and contact control. In the case of using a soft, low modulus contact partner or flexible structural elements, friction can be increased. Controlled relaxation of the adhesive bond can be achieved analogously to the gecko's foot by deliberate deformation of the structure. In contact with granular materials, friction can be increased by increasing the blocking effect by adjusting the shape of the grains and structure [L. 7–9].

To minimize the rapid wear of a structure, elastomers are more suitable than thermoplastics. The wear of elastomers in smooth contacts occurs due to fatigue processes. When an adhesive sliding contact deforms, it generates tensile strains that drive a fatigue crack network. The spreading energy of two lubricated contact partners was described by Israelachvili. Wu-Bavouzet described a characteristic speed for forced wetting corresponding to the elastic length of the closed contact and the contact radius of hard partners [L. 10, 11].

Wu-Bavouzet et al. conducted a systematic study on the formation of friction on elastomers in contacts with smooth surfaces. They found that the wear of elastomers in smooth contacts is described by fatigue processes, which are driven by tensile strains generated by the deformation of an adhesively sliding contact. The effect of surface elasticity, interfacial energies, and viscosity on the formation of continuous or stick-slip-dominated gliding was described by the authors. Dry contacts exhibit at least three different velocity regimes. At low speeds, thermal fluctuations cause the formation of the adhesive bond and result in continuous gliding. At higher speeds, a minimum of the frictional force versus velocity is generated due to the energetic equivalency of elastic strain and adhesion. At higher velocities, a cyclic tearing off from the adhesively formed contact occurs, leading to a reduction in the pronounced contact surface and a slip movement until a bonding or stick phase occurs again. The elastic length that is overcome until a slip phase occurs again is described by the ratio of interfacial energies and shear elasticity. The ratio of this length and the mean slip velocity is a characteristic time that is important for deriving further mechanisms. Wu-Bavouzet et al. also found that at higher speeds, continuous sliding is achieved. Additionally, the authors described the basic contact between elastomer and hard body as the elastomer being lifted by the pressure in the form of a lip, which develops as a wave in or around the contact [L. 11–14].

The addition of hBN (hexagonal boron nitride) to the silicone matrix is aimed at improving the tribological properties, i.e. reducing friction and material wear under high load and temperature conditions. In addition, hBN can increase the wear resistance of the material, as well as improve thermal and insulating properties. Applications for these types of materials can span many fields, including the mechanical industry, aerospace, aerospace, chemical industry as well as biomedicine. HBN was characterized by Lipp et al. [L. 15], while the self-lubricating properties of hBN were confirmed by Kuang et al. [L. 16]. The Si3N4 along with hexagonal boron nitride (hBN) composite was

investigated against alumina for improving wear rate using Taguchi method. A pin on disk wear test in a combination of an Si3N4-hBN composite and an Al2O3 counter-sample was investigated and the results showed that 8% hBN in Si3N4 showed minimal weight loss [L. 17]. Adding titanium to silicones can affect their properties, such as hardness, mechanical strength, abrasion resistance, UV resistance, and tribological properties. For example, the results published by Vaimakis-Tsogkas, D.T et al. describe the effect of the addition of Ti02 on the tribological and mechanical properties of silicone-based composites [L. 18]. Nguyen et al. addressed a topic involving the effect of TiO2 nanocomposites on the properties of polyethylene [L. 19].

The aim of the study was to investigate the effect of different additives (hBN and Ti) on the mechanical and tribological properties of silicone. The study aimed to determine the changes in Young's Modulus, stresses, elongation, and hardness values of the silicone samples containing different compositions of the additives. Additionally, the study aimed to determine the changes in the contact area, maximum and average contact pressures, maximum shear stress, and depth at which maximum shear stress occurs. Furthermore, the study aimed to evaluate the tribological properties of the silicone samples by measuring the coefficient of friction (COF) during the tribological tests. The objective of the study was to determine the optimal composition of the additives that would improve the mechanical and tribological properties of silicone.

MATERIALS AND METHODS

Materials

The samples were made on the basis of GUMOSIL® AD-1S silicone by Zakład Chemiczny "Silikony Polskie" Sp. z o. o. (for convenience, in the following points marked as "Si"). It is a liquid two-component silicone elastomer, which, under the influence of a catalyst, hardens by addition, creating flexible models with very good strength parameters, faithfully reproducing the texture of the model (minimal linear shrinkage) and with good thermal resistance. It withstands long-term heating at temperatures up to 150°C and short-term up to 180°C. It is approved for use in food [L. 20].

The silicone (Si) matrix samples were reinforced with hexagonal boron nitride (hBN) or titanium (Ti) in various mass fractions (Table 1). These additives were used due to their properties – high hardness, abrasion resistance, dimensional stability under the influence of temperature, and resistance to chemical compounds. Additionally, hBN has lubricating properties which may affect surface wear.

Table 1. Content of additives in tested samples.
Tabela 1. Zawartość dodatków w badanych próbkach

Notation	Quantity of additive [%]		
	Si	Ti	hBN
Si	100	-	-
hBN2	98	0	2
hBN11	89	0	11
Ti13	87	13	0
Ti23	77	23	0

The powders were purchased from ABCR Gmbh. According to the manufacturer, the content of Ti was 99.7% wt., while hBN 99% wt.; 0.3% wt. and 1% wt., respectively, were impurities. The morphology of the powders was confirmed and the results will be published in the Materials journal [L. 21].

Samples preparation

The samples for friction and strength tests were prepared by heating in an oven at 100 ◦C for 60 minutes. Previously prepared mixtures of materials (in appropriate proportions) were mixed, then deaerated, molded and placed in the furnace. The molds made it possible to produce round samples with dimensions of 30 mm x 5 mm (diameter x height) and boats with dimensions in accordance with the standard. After the required time, they were taken out of the kiln and the cooling process began, which lasted 24 hours. The samples were then finished.

Young's Modulus

The static tensile test was carried out on a Zwick/Roell Z010 testing machine (ZwickRoell, Wrocław). The average value of 5 measurements was presented as the measurement result.

Hardness Test

The hardness of the samples was measured using a Shore A Durometer (VEB, Werkstoffprufmaschinen

Leipzig). The measurements were taken approximately 3 mm apart on the surfaces of the samples. The average value of 10 measurements was presented as the measurement result.

Geometry of Contacting Elastic Body

In addition to the use of advanced technology, a lot can be learned by calculation – with the use of parameters such as the load, expressed below as W [N], and the radius of the measuring ball R [m], it is possible to obtain the stress values appearing during the test itself. These calculations can be based on the formulas given by Stachowiak [L. 22]:

$$\frac{1}{R_x} = \frac{1}{R_{ax}} + \frac{1}{R_{bx}} \qquad (1)$$

$$\frac{1}{R_y} = \frac{1}{R_{ay}} + \frac{1}{R_{by}} \qquad (2)$$

where R_{ax} and R_{ay} are the radius of curvature of the measuring ball, so they are equal. R_{bx} and R_{by} refer to the curvature of the surface of the tested object, which in the case described means approximately infinity.

Such a relationship satisfies the condition $\frac{1}{R_x} = \frac{1}{R_y}$, allowing the use of the formula for the reduced radius of curvature:

$$\frac{1}{R'} = \frac{1}{R_x} + \frac{1}{R_y} \qquad (3)$$

The reduced Young's Modulus described in the work of N'Jock is needed for further tests [L. 23]:

$$\frac{1}{E'} = \frac{1-v_1^2}{E_1} + \frac{1-v_2^2}{E_2} [MPa] \qquad (4)$$

where: v_1, v_2 – Poisson's ratio for material 1 and 2,
E_1, E_2 – Young's Modulus of material 1 and 2 [MPa].

The data allow the determination of the contact area between the measuring ball and the test sample:

$$a = \left(\frac{3WR'}{E'}\right)^{\frac{1}{3}} [m] \qquad (5)$$

where: W – normal load [N].

And then the maximum and average pressure on the object:

$$P_{max} = \frac{3W}{2\pi a^2} [MPa] \qquad (6)$$

$$P_{average} = \frac{W}{\pi a^2} [MPa] \qquad (7)$$

Maximum deflection:

$$\delta = 1.0397 \left(\frac{W^2}{E'^2 R'}\right)^{\frac{1}{3}} [m] \qquad (8)$$

Maximum shear stress:

$$\tau_{max} = \frac{1}{3} P_{max} [MPa] \qquad (9)$$

Depth at which maximum shear stress occurs:

$$z = 0,638a [m] \qquad (10)$$

Thanks to the values obtained in a computational way, it is possible to simulate the loads to which the samples were subjected during tribological tests and adapt them to the strength of the tested materials.

Tribological tests

Tribological tests were carried out on a BRUKER UMT2 Tribolab tester (Bruker Corporation, Billerica, MA, USA), operating in a pin-on-flat configuration under reciprocation displacement, and an original tribotester in pin-on-disk configuration. The samples were examined in accordance with the applicable standards (ASTM G99). The tests were conducted for a combination of a ŁH15 steel ball (a diameter of 10 mm and a roughness of Ra = 0.6 μm) and a sample with a silicone matrix. No lubricant was used. The tests were carried out at a temperature: 20 ± 5°C, relative humidity: 50 ± 5%, and with the maximum load range: 200 N. Additionally, abrasion products were not removed from the contact zone.

The tests were carried out for a pressure force of 5 N, a movement speed of 25 mm/s and a time of 30 min. In the case of two-way traffic, the measuring section was 30 mm, and the tests resulted in, among others, the COF waveform. The methodology of test was described by Czapczyk et al. [L. 24].

Coefficient of friction was assessed using formula (1) [L. 24]:

$$\mu = (A\_r\,\tau)/W \qquad (11)$$

where μ is the coefficient of friction, A_r is the real contact area, τ is the effective shear strength of contacts, and W is the normal load (N).

For the purpose of the tests employing these methods, the tribotesters were equipped with a fixed and rotating table. The samples were clamped, which allowed their   during the measurement. **Figure 1** presents a ball-on-plane tribotester in one-way rotational motion manufactured at the Institute of Mechanical Technology at the Poznań University of Technology.

The study was conducted for three samples of each composite. Each composite was measured in at least five parallel experiments to ensure adequate statistical evaluation. Two outlier measurements were removed. The average value of the coefficient of friction for individual samples is presented with the appropriate standard deviations.

Optical microscopy

Detailed observations were made using an Alicona Infinite Focus UR-10 optical profilometer (Bruker Alicona, Graz, Austria). The examination allowed the analysis of the specific deformation of the dynamically charged surface of the samples and the explanation of the mechanism of wear; it also helped obtain an average track profile. In addition, width and depth measurement is possible.

RESULTS AND DISCUSSION

Hardness Measurements and Young's Modulus

The fabricated materials were subjected to a static tensile test and hardness measurement. The values of Young's Modulus, stresses and elongation are presented in **Table 2**. In the case of the addition of titanium, the values of Young's Modulus and stresses increase. The addition of hBN causes a decrease in these values, and a significant increase in the case of hBN11. In the case of the addition of Ti, the Young's Modulus reaches values twice as high as when hBN is added. For samples with a low content of additives (hBN2 and Ti13) and pure silicone, the elongation value was similar. The highest stresses occurred for hBN11 (0.362 MPa) and Ti23 (0.553 MPa).

The hardness values of the investigated samples are presented in **Figure 2**. An increase in
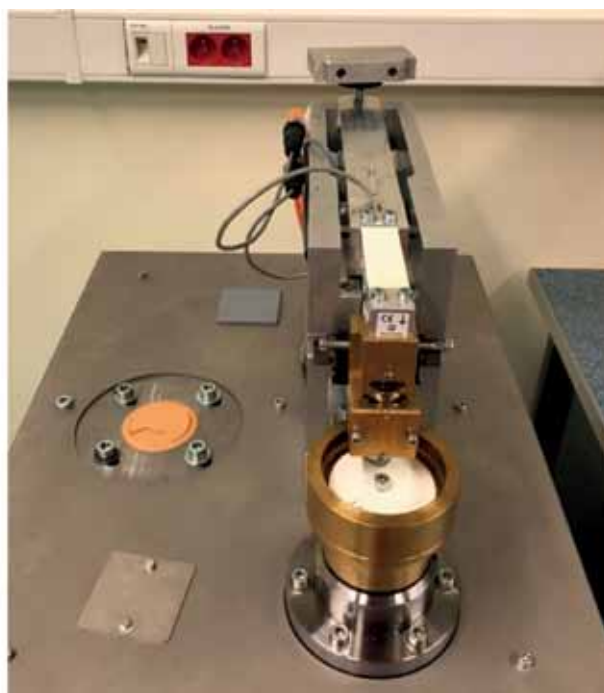
Fig. 1.　Original ball-on-plane tribotester in one-way rotational motion manufactured at the Institute of Mechanical Technology at the Poznań University of Technology

Rys. 1.　Oryginalny tribotester kulka–płaszczyzna o jednokierunkowym ruchu obrotowym wyprodukowany w Instytucie Techno-logii Mechanicznej na Politechnice Poznańskiej

Table 2. Static tensile test results
Tabela 2. Wyniki statycznego testu rozciągania

Notation	Young's Modulus [MPa]	Strain stress in the x-axis [MPa]	Elongation [%]
Si	1.14	0.18	330
hBN2	1.08	0.19	310
hBN11	2.98	0.36	230
Ti13	2.03	0.28	320
Ti23	5.43	0.55	190

the Shore A values, depending on the Ti and hBN content, is clearly noticeable. The additives caused a significant increase in hardness. Higher values cane be observed for titanium.
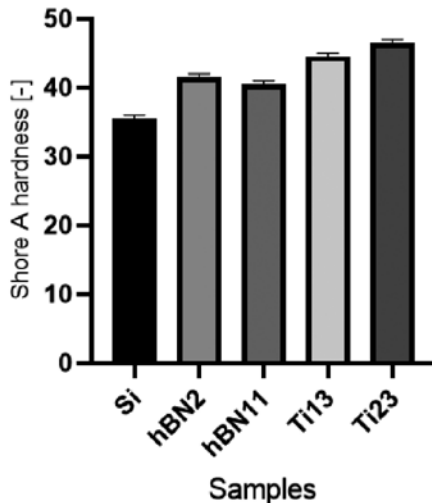
Fig. 2. Shore A hardness of the samples with various content
Rys. 2. Twardość Shore'a badanych próbek z różną zawartością dodatku

Positive hBN caused an increase in hardness by about 14%, while Ti by about 28%. With the increase in the hBN content, the hardness value slightly decreased, while in the case of Ti it increased. This trend is shown in **Figure 3**.

Geometry parameter calculations of contacting elastic body

The article explores the influence of contact geometry on the wear mechanisms of the tested composites. This is a fundamentally important aspect because a properly designed contact geometry can significantly impact the durability and performance of materials during their use. **Table 3** presents calculations made for the composite-steel pair. The values were computed for tests conducted under a pressure of 5 N with a ball with a radius of 10 mm.

One of the significant conclusions drawn from the conducted calculations is that even minor changes in the composite's composition have a substantial effect on the contact surface. The addition of hBN increases the contact surface by 15%, which can be advantageous due to a more even
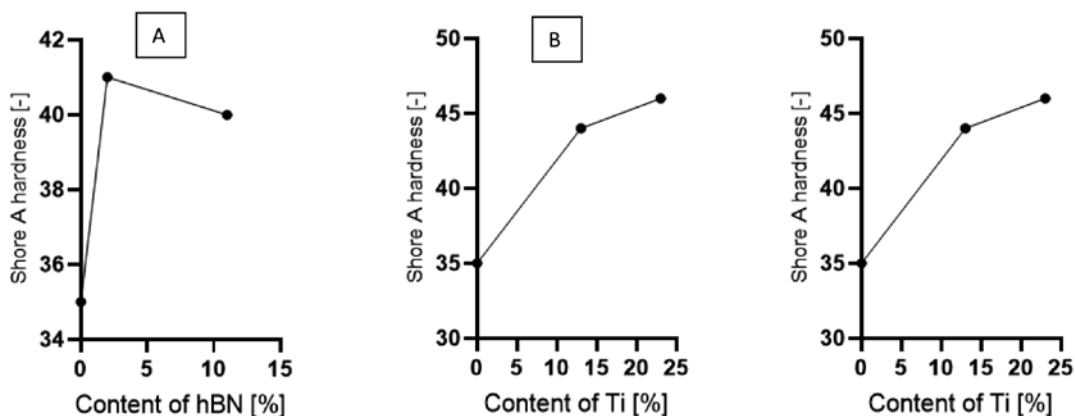
Fig. 3. Shore A hardness as a function of hBN for samples containing: A: hBN and B: Ti.
Rys. 3. Twardość Shore'a w funkcji hBN dla próbek zawierających: A: hBN i B: Ti

distribution of load and lower maximum contact pressures. With an increase in the hBN content, the contact area decreases by 16% compared to Si, while maximum contact pressures rise. On the other hand, the addition of Ti leads to a 31% reduction in the contact surface, concentrating forces on a smaller area, resulting in higher local stresses. An increase in the Ti content leads to higher maximum contact pressures (by 173%).

It is essential to take note of the Maximum Shear Stress parameter, which also undergoes changes, depending on the contact geometry.

Additions of hBN and Ti influence the increase in this parameter with an increase in their content. This means that a higher quantity of these additives can increase stresses in the contact area, which can affect the material wear process.

Furthermore, it is worth mentioning the depth at which the maximum shear stress occurs, which can be significant for material durability. The highest value was observed for hBN2, while the lowest was noted for Ti23. Deeper maximum shear stresses can lead to more significant material wear in specific contact areas.

Table 3. Geometry parameter calculations of contacting elastic body
Tabela 3. Obliczenia parametrów geometrycznych powierzchni stykającego się ciała elastycznego

Notation	Force	Diameter	Contact area dimensions	Maximum contact pressures	Average contact pressures	Maximum deflection	Maximum shear stress	Depth at which maximum shear stress occurs
	F [N]	d [mm]	a [μm]	Pmax [MPa]	Pavg [MPa]	δ [μm]	τmax [MPa]	z [μm]
Si	5	10	579.4	7.1	4.7	573.8	2.4	369.7
hBN2	5	10	666.5	5.4	3.6	759.3	1.8	425.2
hBN11	5	10	489.9	9.9	6.6	410.3	3.3	312.6
Ti13	5	10	550.2	7.9	5.3	517.4	2.6	351.1
Ti23	5	10	403.4	14.7	9.8	278.1	4.9	257.3

Evaluation of Tribological Properties

Two-way traffic

The charts of changes in the coefficient of friction were obtained automatically from tribological tests using the computer software embedded in the BRUKER UMT TriboLab device. For all samples, the value of the coefficient of friction was stabilized (**Figure 4**).

The courses of COF changes as a function of time for samples with different content of the additive are comparable, however, in the case of samples containing hBN, the maximum value is reached after a longer time compared to samples containing Ti; with longer operation, COF decreases. This is characteristic of more flexible samples. In the case of samples containing hBN and Ti, the COF value decreases with increasing content of additives. The hBN11 and Ti23 samples reach a value of approx. 1, while hBN2 and Ti13 approx. 1.2.
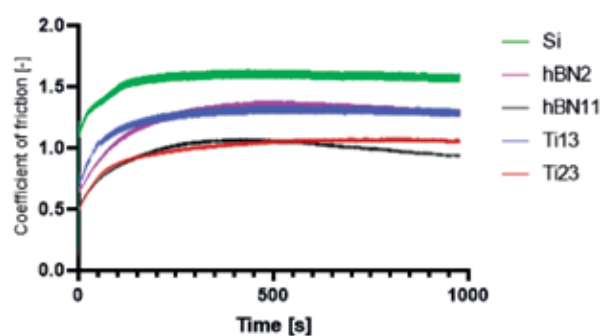
Fig. 4. Coefficient of friction as a function of time for the samples for the normal load of 5 N
Rys. 4. Współczynnik tarcia w funkcji czasu dla próbek o obciążeniu normalnym 5 N

Analyzing the graph (**Figure 5**) showing the value of the friction coefficient as a function of the content of hBN. With the increase in the content of additives, the COF value decreases. In the case of hBN, an increase in the content by 9% caused a decrease in the COF value by 28%, while an increase in the content by 10% decreased by 17% compared to the higher value.
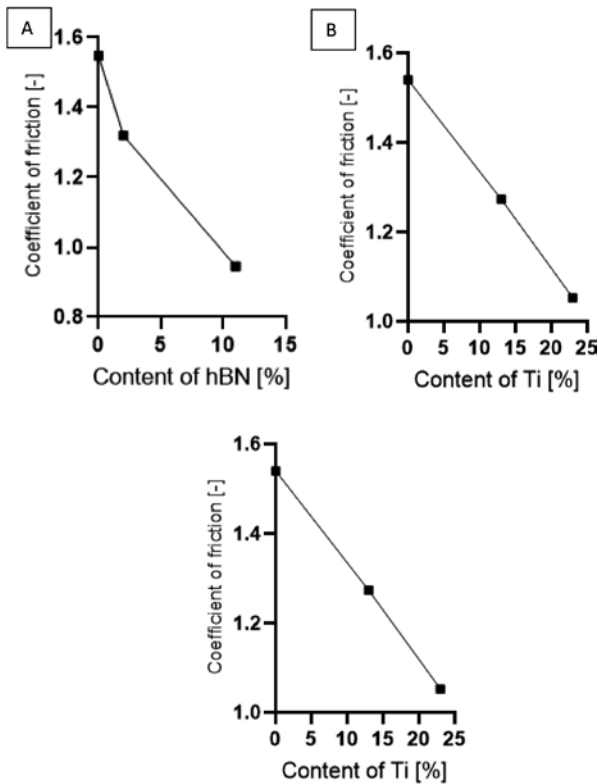
Fig. 5.   Steady state values of the coefficient of friction of the composite samples with various additives.

Rys. 5.   Ustabilizowane wartości współczynnika tarcia próbek kompozytowych z różnymi dodatkami

Fig. 6.   Steady state values of the coefficient of friction of the Si samples with various additives tested on the original tribotester

Rys. 6.   Ustabilizowane wartości współczynnika tarcia próbek Si z różnymi dodatkami testowane na oryginalnym tribotesterze

Fig. 7.   Comparison of the value of the averaged coefficient of friction after stabilization for tribotesters: B – Bruker UMT2. T – Original Tribotester

Rys. 7.   Porównanie wartości uśrednionego współczynnika tarcia po ustabilizowaniu dla tribotesterów: B – Bruker UMT2. T – Oryginalny Tribotester

One-way traffic

The charts of changes in the coefficient of friction were obtained automatically from tribological tests using the computer software embedded in the original tribotester. For all samples, the value of the COF was stabilized.

Figure 6 presents the steady state values of the coefficient of friction of the Si samples with various additives. The addition of hBN and Ti to Si resulted in an decrease in the COF value. With the increase in the content of additives, the COF value decreases. With the increase of the hBN and Ti content, the COF value decrease. The lowest value was recorded for a sample containing 11% of hBN, while the highest for samples with 2% of hBN.

Below (**Figure 7**) is a summary of the results obtained during tests carried out under various conditions on various tribotesters. In both cases (two-way and one-way traffic), the averaged COF values are similar. The values obtained from the Bruker measuring device are usually lower by approx. 10-15%, which may be due to the presence of the braking distance.
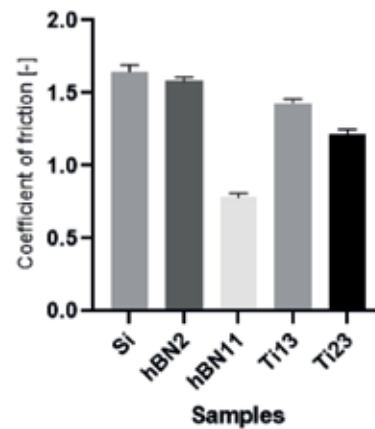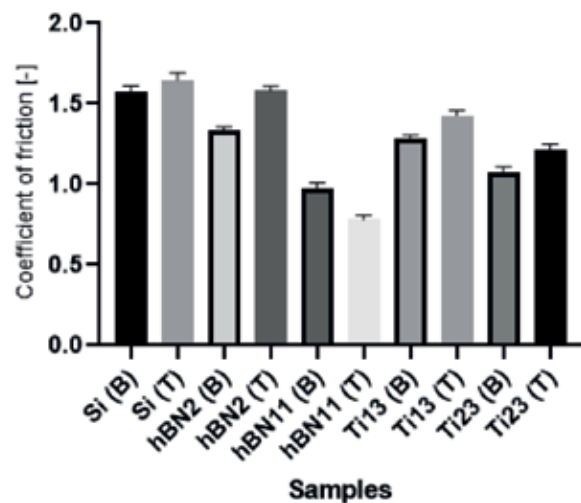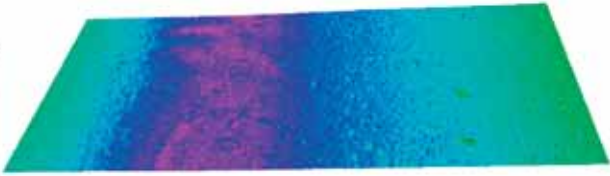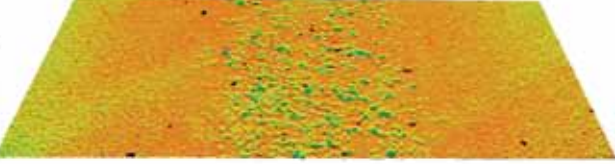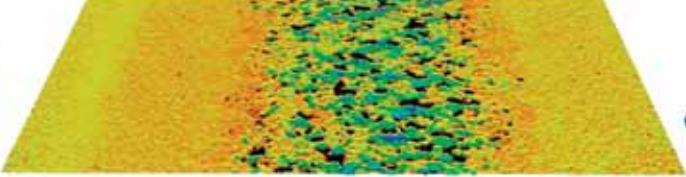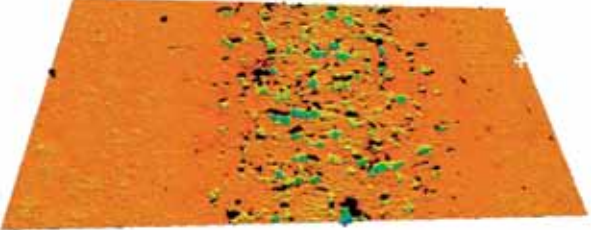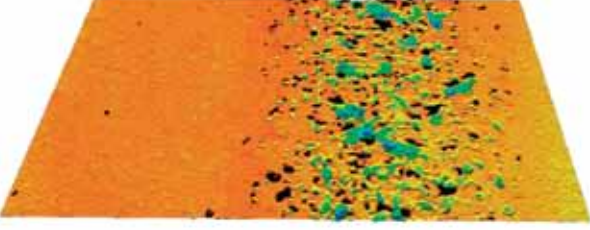
Microscope observation

After the tribological tests were carried out, microscopic observations were performed on an Alicon focal differentiation microscope. The results are presented in **Table 4**. In the case of silicone, there are high adhesive forces. Between the ball and the sample, the material exfoliates, deforms elastically. In the case of the hBN additive, the self-lubricating properties are observed, while in the case of the Ti additive, particle is crushed and the adhesive forces are lower than in the case of pure silicone.

Table 4.   **Comparison of the friction area observed under an Alicona focal differentiation microscope**

Tabela 4.   Porównanie obszaru tarcia obserwowanego pod mikroskopem różnicowania ognisk Alicona

Notation	Microscopic observation
Si	
hBN2	
hBN11	
Ti13	
Ti23	

Figure 8 shows the wear track profile for all tested samples. In the case of the samples with additives, slight surface wear was observed, and the obtained profile is jagged. This is due to the low hardness and high Young's Modulus value. In addition, the crack profile is affected by the crumbling particles of additives.

Table 5 shows the values of the geometric parameters of the wear track (width and depth). Values were averaged from 1,000 profiles. A significant depth difference between pure silicone (up to 22.61 µm) and with additives can be observed – additives reduce the width and depth of the track profile. In the case of the hBN addition, the

path width decreases and the depth increases with increasing content. This may be due to the effect of lubricating properties and increase in hardness. The addition of Ti resulted in the opposite tendency – with the increase in the content, the width and depth of the path track increase.
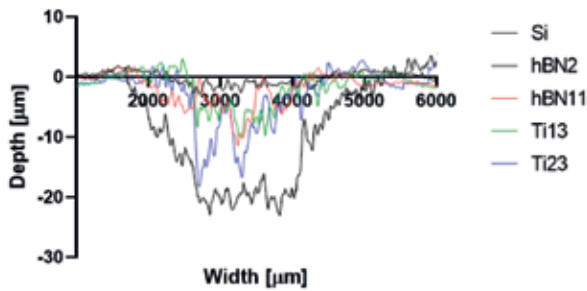

Fig. 8.   Wear track profile for all tested samples
Rys. 8.   Profil śladu zużycia dla wszystkich badanych próbek

Table 5.   Geometrical parameter of the wear track profile
Tabela 5. Parametr geometryczny profilu śladu zużycia

Notation	Width [mm]	Depth [μm]
Si	3.4	22.6
hBN2	3.0	3.7
hBN11	2.2	10.9
Ti13	2.0	9.1
Ti23	3.4	17.6

Figure 9 shows the change in the width and depth values for the tested materials. The additions of hBN and 13% of Ti cause a decrease in the width value, while 23% of Ti causes an increase. As the hBN content increases, the width decreases and the depth increases. The additions of Ti and hBN cause a significant decrease in depth, which increases with increasing content.

Two sets of changes in the COF value relative to Shore A hardness (**Figure 10A**) and Young's Modulus (**Figure 10B**) are presented below. It was noticed that in the case of the hBN addition, the COF value decreases, regardless of the hardness changes, while in the case of the Ti addition, the increase in the COF value is directly proportional to the content of the additive and inversely proportional to the hardness. From the analysis of **Figure 10B** it follows that the additions cause an increase in the Young's Modulus value while reducing the COF value.
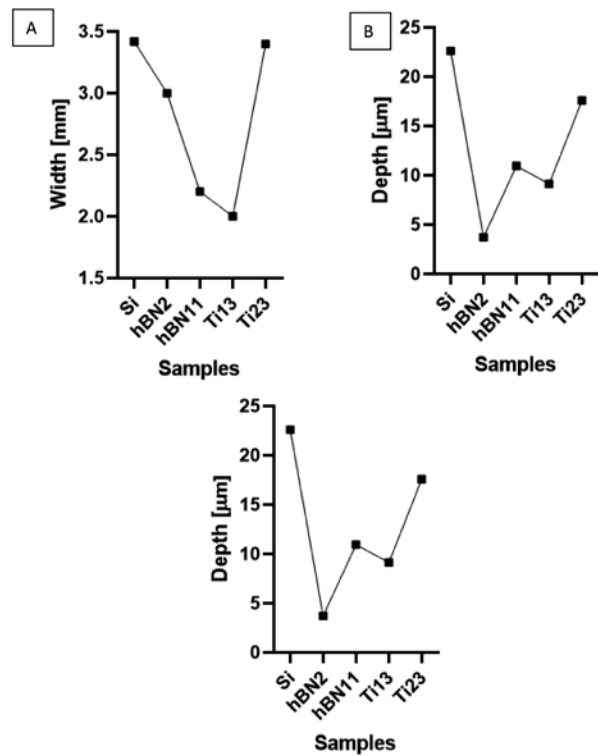

Fig. 9. TC change in the width and depth values for the tested materials
Rys. 9.   Zmiana temperatury krytycznej w wartościach szerokości i głębokości dla badanych materiałów
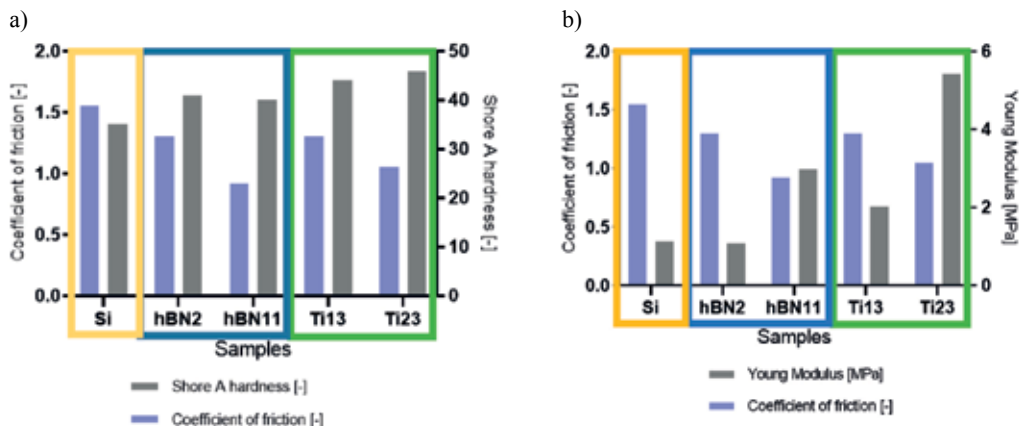

Fig. 10. Tables of changes in COF values relative to Shore A hardness (A) and Young's Modulus (B)
Rys. 10. Tabele zmian wartości COF względem twardości Shore'a (A) i modułu Younga (B)

CONCLUSIONS

The following conclusions can be drawn from the conducted research:

- The addition of titanium and heksagonal boron nitride to silicone significantly affects its mechanical properties, including the Young's Modulus, stress, and hardness. The addition of Ti generally increases these parameters, while the addition of hBN may lead to a decrease, except for sample hBN11, where a significant increase in the Young's Modulus was observed.
- Regarding tribological properties, the coefficient of friction decreases as the content of additives, both hBN and Ti, increases. Samples hBN11 and Ti23 exhibit the lowest values of this coefficient.
- The geometric configuration of the contact has a significant impact on the contact area and contact pressures. The addition of hBN increases the contact area, which can be beneficial for even load distribution and a reduction in contact pressures. On the other hand, the addition of Ti leads to a decrease in the contact area, concentrating forces on a smaller surface, resulting in higher local stresses.
- The parameter of shear stress also changes depending on the contact geometry. The addition of hBN and Ti influences an increase in this parameter with the increasing content of these additives.
- The depth at which shear stress occurs is crucial for material durability. The highest values of this parameter were observed for samples with the addition of hBN2 and the lowest for samples with the addition of Ti23. Deeper shear stresses can lead to more significant material wear in specific contact areas.
- Additives also affect the material's hardness, significantly increasing it, with a more considerable increase in the case of titanium addition.
- Microscopic observations confirm that additives have a significant impact on the surface behaviour and microstructure of the material during tribological tests.

The ultimate conclusion is that the careful dosing and control of additive content in silicone composites are crucial to achieving the desired mechanical and tribological properties for specific applications. Additionally, the geometric contact configuration plays a significant role. Microscopic observations help understand wear mechanisms and the impact of additives on these mechanisms.

REFERENCES

1. Schallamach A.: How does rubber slide? Wear 1971, 17, 301–312.
2. Liu Y., Li J., Yi S., Ge X., Chen X., Luo J.: Enhancement of friction performance of fluorinated graphene and molybdenum disulfide coating by microdimple arrays. Carbon 2020, 167, pp. 122–131.
3. Nosal S.: Tribology. Introduction to the issues of friction. wear and lubrication. Poznan 2012.
4. Tramsen H.T., Gorb S.N., Zhang H., Manoonpong P., Dai Z., Heepe L.: Inversion of friction anisotropy in a bio-inspired asymmetrically structured surface. J. R. Soc. Interface 2018, p. 15, 20170629.
5. Tramsen H.T., Heepe L., Homchanthanakul J., Wörgötter F., Gorb S.N., Manoonpong P.: Getting grip in changing environments: The effect of friction anisotropy inversion on robot locomotion. Appl. Phys. A 2021, 127, pp. 1–9.
6. Scherge M., Gorb S.: Biological Micro-and Nanotribology: Nature's Solutions; Springer: Berlin, Germany; London, UK, 2011
7. Wu W., Lutz C., Mersch S., Thelen R., Greiner C., Gomard G., Hölscher H.: Characterization of the microscopic tribological properties of sandfish (Scincus scincus) scales by atomic force microscopy. Beilstein J. Nanotechnol. 2018, 9, pp. 2618–2627.
8. Schneider J., Djamiykov V., Greiner C.: Friction reduction through biologically inspired scale-like laser surface textures. Beilstein J. Nanotechnol. 2018, 9, pp. 2561–2572.
9. Fukahori Y., Sakulkaew K., Busfield J.: Elastic–viscous transition in tear fracture of rubbers. Polymer 2013, 54, pp. 1905–1915
10. Intermolecular and Surface Forces, Israelachvili Jacob N., Elsevier Ltd. Oxford, 2011
11. Wu-Bavouzet F., Clain-Burckbuchler J., Buguin A., De Gennes P.-G., Brochard-Wyart F. Stick-Slip: Wet Versus Dry. J. Adhes. 2007, 83, pp. 761–784.

12. Fukahori Y., Gabriel P., Busfield J.: How does rubber truly slide between Schallamach waves and stick–slip motion? Wear 2010, 269, p. 854–866.
13. Rand C.J., Crosby A.J.: Insight into the periodicity of Schallamach waves in soft material friction. Appl. Phys. Lett. 2006, 89, p. 261907.
14. Rand C.J., Crosby A.J.: Friction of soft elastomeric wrinkled surfaces. J. Appl. Phys. 2009, 106, p. 064913.
15. Lipp A., Schwetz K.A., Hunold K.: Hexagonal Boron Nitride: Fabrication, Properties and Applications. Journal of the European Ceramic Society. 1988.
16. Kuang W., Zhao B., Yang C., Ding W.: Effects of h-BN particles on the microstructure and tribological property of self-lubrication CBN abrasive composites. Ceramics International. 2019, 46(2).
17. Ghalme S., Mankar A., & Bhalerao Y.: Optimization of wear loss in silicon nitride (Si 3 N 4)–hexagonal boron nitride (hBN) composite using DoE–Taguchi method. SpringerPlu 2016 s, 5(1), 1671.
18. Vaimakis-Tsogkas D.T., Bekas D., Giannakopoulou T., Todorova N., Paipetis A.S. Barkoula N.: Effect of TiO2 addition/coating on the performance of polydimethylsiloxane-based silicone elastomers for outdoor applications. Materials Chemistry and Physics 223. 2019.
19. Nguyen G., Thai H., Mai D., Tran H.T., Lam T., Vu T.: Effect of titanium dioxide on the properties of polyethylene/TiO2 nanocomposites. Composites Part B: Engineering. 2013, 45, pp. 1192-1198.
20. https://www.sklep.silikonypolskie.pl/gumosil-ad-1s-opak-v-1,3,9049,9042.
21. Wierzbicka N.,Talar R., Grochalski K., Piasecki A., Węgorzewski M., Reiter A.: The friction of the composite based on polyethylene with inorganic additives. Materials. 2023. 16, p. 14.
22. Stachowiak, G., Batchelor A. W. Engineering tribology. 2013, Butterworth-Heinemann.
23. N'Jock M.Y., Roudet F., Idriss M., Bartier O., Chicot D.: Work of indentation coupled to contact stiffness for calculating elastic modulus by instrumented indentation. Mechanics of materials. 2015, 94.
24. Czapczyk K., Zawadzki P., Wierzbicka N., Talar R.: Microstructure and Properties of Electroless Ni-P/ Si3 N4 Nanocomposite Coatings Deposited on the AW-7075 Aluminum Alloy. Materials. 2021, 14, 4487.